This article has been accepted for publication in IEEE Transactions on Antennas and Propagation. This is the author's version which has not been fully edited and content may change prior to final publication. Citation information: DOI 10.1109/TAP.2024.3486452

A High-Gain Pattern and Beamwidth Reconfigurable Dielectric Resonator Antenna based on Parasitic Metal Panels

Daotong Li, *Senior Member, IEEE*, Lanlan Yang, Linsong Shi, Jiaxin Wang, Ying Liu, Naoki Shinohara, *Senior Member, IEEE*, and Qiang Chen, *Senior Member, IEEE*

***Abstract*—In this paper, a novel pattern and beamwidth reconfigurable cylindrical dielectric resonator antenna (CDRA) is proposed. The pattern reconfigurable structure is achieved by a pair of 3D-printed arc-shaped parasitic metal panels, which are capable of high-gain beam scanning with ±24° in the H-plane and ±18° in the E-plane radiation, respectively, without the electrical controlling components. Moreover, by arranging the arc-shaped parasitic metal panels symmetrically, the half-power beamwidth (HPBW) of the antenna can be adjusted from 48° to 79°. The proposed DRA utilizes a stacked multi-layer dielectric substrate structure to excite the $HEM_{12\sigma}$ higher order mode which improves the gain performance. Finally, the antenna achieved the maximum gain of 10.6dBi in the operating bandwidth. The pattern reconfiguration through mechanical control avoids the extra insertion loss that could result from PIN diodes, and allows for a high overlapped bandwidth in different radiation patterns. The measured overlap-operating frequency band and maximum gain of the antenna with different radiation states are 2.17-2.72GHz (fractional bandwidth of 22.49%) and 10.42dBi, respectively. These values are well suited for the 2.4GHz ISM band applications.**

Index Terms—**pattern reconfigurable, beamwidth reconfigurable, dielectric resonator antenna, high gain, ISM band**

I. Introduction

With the rapid development of the wireless communication systems, many pattern-reconfigurable antennas have been developed to provide better radiation performance and avoid noise source or electronic jamming [1]-[5]. Different from traditional phased arrays, pattern-reconfigurable antennas tend to have the advantages of simple structure, small size, low cost, and it is possible for pattern-reconfigurable antenna to control the beam by a single antenna [6]-[8]. Notably, pattern-reconfigurable antennas with directional radiation have been developed in many applications, such as tunnel and vehicular environments due to a good directivity. However, these antennas also have some drawbacks such as complex structures or controlling strategy.

Pattern reconfigurable dielectric resonator antenna (DRAs) typically use multiple feeding structures and switch network to control beam pattern [9-16]. In [9], a passive four-element DRA array is verified to achieve a wide 3 dB scan coverage of ±105°, the maximum gain of the scanning beam (10.8 dBi) is located at the off-axis angle of ±66°. However, the proposed DRA arrays have an impedance bandwidth only of 3.33%, and introduce additional power splitter and phase shifter networks, which lead to a complex feeding mechanism. In [10], a pattern reconfigurable high-gain spherical DRA was proposed, which has three switching states to control the radiation pattern of ±28° and 0°. It achieves a maximum gain of 9.12 dBi, but the overlapped bandwidth is only 1.7%. A pattern-reconfigurable DRA that is controlled by pin diodes in Ref. [11], providing an omnidirectional radiation pattern and two unidirectional endfire patterns in the azimuthal plane [11]. However, the peak gain in endfire status only reaches 4.5 dBi. In [12], the proposed DRA realized an omnidirectional radiation pattern and boresight patterns with orthogonal polarizations (horizontal plane). A central DRA and two parasitic liquid DRAs are combined in [13], similarly, omnidirectional and unidirectional radiation can be realized, and polarization reconfiguration can be achieved under endfire status. The low maximum gain of the antenna is 5 dBi because the HEM_{113} fundamental mode is excited. Since the DRA dose not excite the higher order mode, the maximum gains of the antenna in literature [12-13] are less than 6.4 dBi. In [14], a switchable high gain dielectric resonator antenna array which achieves maximum gain and steering angle of 12.8 dBi and ±30° is proposed, but the 6-element antenna array has a large size. A pattern-reconfigurable DRA with endfire beam-scanning feature is proposed in [15], which consists of a DR, a switchable director with 10 pin diodes, and a differential feeding structure. The proposed antenna enables a near-continuous beam scanning from −48° to +48° in the azimuth plane. But the overlapped bandwidth is only 2.08%. In [16], a pattern-reconfigurable antenna with three switchable radiation patterns based on diodes control is investigated. the radiation pattern of the antenna can be switched between the omnidirectional, broadside, and unilateral modes. Similarly, the overlapped bandwidth for different states is 7.3% and the gain for the unilateral mode is 5.18 dBi.

In this paper, a novel pattern and beamwidth reconfigurable high gain CDRA based on the arc-shaped parasitic metal panels is proposed and experimentally verified. It consists of a CDRA with a multi-layer dielectric combination, the slot coupling structure, microstrip line transition and a pair of arc-shaped parasitic metal panels. The radiation pattern of the CDRA can be controlled by adjusting the position of the arc-shaped parasitic metal panels mechanically. When two arc-shaped parasitic metal panels are spliced together on the side and front of the CDRA, the radiation patterns of the CDRA realize the steering angle of ±24°/±18° in the H/E plane [17]. Meanwhile, in order to achieve high gain performance, the antenna adopts the multi-layer dielectric to excite the $HEM_{12\sigma}$ higher order mode. The CDRA achieves the maximum gains of the 8.52 dBi/10.5 dBi in the ±24° (H-plane)/ ±18° (E-plane). When two arc-shaped parasitic metal panels are placed symmetrically about the antenna, the half-power beamwidth (HPBW) can be adjusted from 48° to 79°.

This work was supported in part by the Chongqing Natural Science Foundation under Grants: CSTB2024NSCQ-MSX1038, CSTB2024NSCQ-MSX1217, in part by the National Natural Science Foundation of China under Grant 61801059, and in part by the Function development project for large and valuable instruments under Grant gnkf2023009. *(Corresponding authors: Daotong Li)*

Daotong Li, Lanlan Yang, Linsong Shi, Jiaxin Wang and Ying Liu are with School of Microelectronics and Communication Engineering, Chongqing University, Chongqing 400044, China.

Daotong Li and Naoki Shinohara are with the Research Institute for Sustainable Humanosphere, Kyoto University, Kyoto 606-8501, Japan.

Qiang Chen is with the Department of Communications Engineering, Tohoku University, Sendai 980-8579, Japan.

Color versions of one or more of the figures in this communication are available online at http://ieeexplore.ieee.org.

This article has been accepted for publication in IEEE Transactions on Antennas and Propagation. This is the author's version which has not been fully edited and content may change prior to final publication. Citation information: DOI 10.1109/TAP.2024.3486452

II. Antenna Design And Investigation

The geometry of the proposed pattern and beamwidth reconfigurable CDRA is shown in Fig. 1(a). This antenna mainly consists of two parts, the first is the high gain CDRA based on higher order mode. The high gain CDRA is realized by stacking multi-layer dielectric which excited the $HEM_{12\sigma}$ higher order mode. The more important contribution of this paper is the pattern and HPBW reconfigurable structure. The pattern and HPBW reconfigurable is realized by using different combinations of arc-shaped parasitic metal panels to interfere with antenna radiation in the *z*-axis direction, so that the CDRA pattern and beamwidth can be switched. Their detailed design and mechanisms are as follows.

A. High Gain Dielectric Resonator Antenna

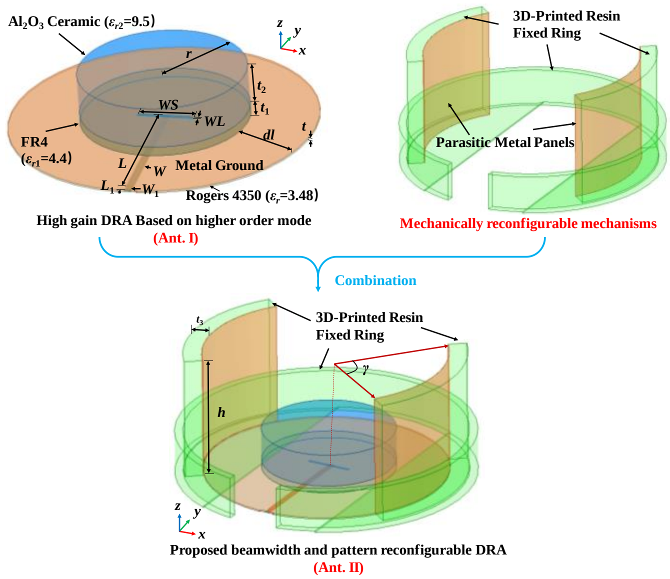

(a)

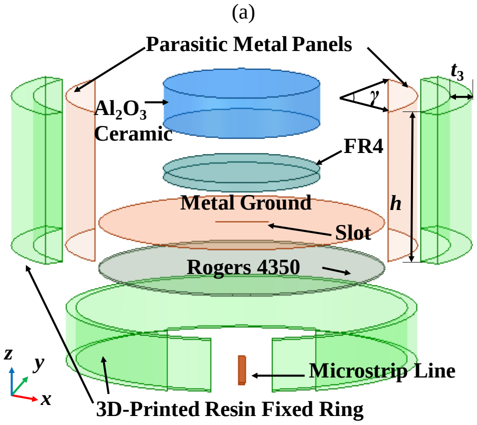

(b)

Fig. 1. Proposed beamwidth and pattern reconfigurable DRA. (a) evolution of proposed beamwidth and pattern reconfigurable DRA, (b) perspective view of the proposed beamwidth and pattern reconfigurable DRA.

Compared with the fundamental mode, exciting the higher order mode of the DRA is a good solution for increasing the realized gain. In this paper, the higher order mode $HEM_{12\sigma}$ is excited by using the multiple stacked DRA. The structure of the proposed high gain CDRA is shown in Fig. 1(b). It consists of CDRA with multi-layer dielectric, ground, slot coupling structure, feeding substrate and microstrip line. The geometry of CDRA, which consists of a substrate layer of FR4 (ε_{r1} =4.4, t_1 =4 mm, r =36 mm) and a substrate layer of 95% alumina ceramic (ε_{r2} =9.5, t_2 =16 mm, r =36 mm). The feeding substrate is composed of Rogers 4350B with the relative permittivity ε_r =3.48, the radius R =65.7 mm, a thickness t =0.762 mm and loss tangent $tan\delta$ =0.004. The feed line adopts the stepped microstrip lines to facilitate impedance matching (W =3.1 mm, L =65.8 mm, W_1 =2.58 mm, L_1 =4.6 mm). The slot aperture (WS =24.2 mm, WL =1.28 mm) is located under the center of the CDRA. The microstrip-to-slot coupling structure is employed to feed and excite the resonant mode of CDRA through the coupling slot structure [18]. The aperture equals to a magnetic dipole, which provides a good impedance matching for the $HEM_{12\sigma}$ mode. Fig. 2(a) shows the impedance bandwidth and maximum gain of the CDRA, and the DRA is attached to the dielectric substrate Rogers 4350B by a low relative permittivity adhesive (3M PR100). It can be seen that the reflection coefficient below -10 dB is 2.34-2.78GHz, fractional bandwidth (FBW) of 17.2%, and the maximum gain of the antenna is 9.16 dBi.

The pattern and beamwidth reconfigurable characteristics of the proposed antenna is implemented by using the parasitic metal panels controlled by AC asynchronous motor, and the speed provided by the motor can fully meet the rotation requirements. As a novel pattern and beamwidth reconfigurable antenna, it can be applied in many potential working scenarios, such as wall-mounted antennas for indoor spaces radiation coverage, and transmitter antennas for microwave wireless power transmission application.

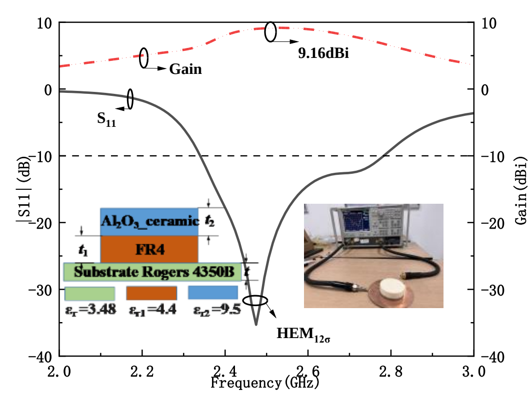

(a)

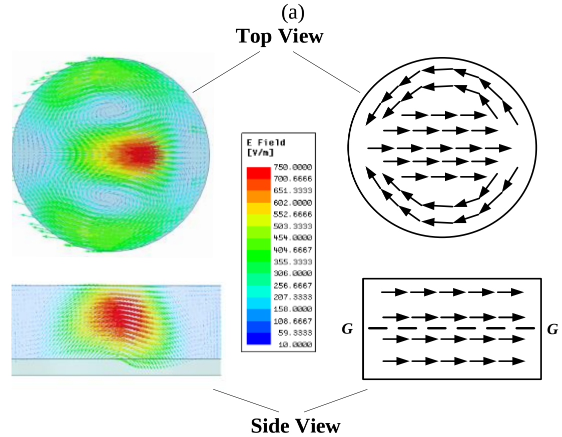

(b)

Fig. 2. Realized gain/S11 and electric field ($HEM_{12\sigma}$ resonant mode) of the aperture-fed multi-layer CDRA. (a) Realized gain and S_{11} (b) Simulated and schematic electric field ($HEM_{12\sigma}$) of CDRA: Top and Side views. (G-G' is the location of the ground plane)

It should be emphasized that the field distribution of the DRA is a useful means to ascertain the excitation of higher order modes [19-

21]. There is an obvious resonant frequency at 2.47GHz, and the excitation of $HEM_{12\sigma}$ higher order mode is determined based on the analysis of the electromagnetic field inside the DRA and the gain performance. As shown in Fig. 2(b), the simulated and theoretical electric field vector distributions of the $HEM_{12\sigma}$ higher order mode in the *xoy* plane shows the existence of two loop electric field distributions, while the electric field vector on both sides is opposite to the electric field vector in the middle, which is almost identical to the schematic diagram. Similarly, *yoz* plane is consistent with schematic diagram in Fig. 2(b).

B Pattern Reconfigurable Antenna Design

The structure of the proposed pattern reconfigurable CDRA is shown in Fig. 1(a). The pattern reconfigurable antenna is controlled by a pair of arc-shaped (R =65.7 mm, γ =37.5°) parasitic metal panels and its thickness t_3 =10 mm, height h =67 mm. It is worth noting that the inner surface of the arc-shaped parasitic metal panel is a copper layer, and the rest of the panel is made of a cheaper resin structure. Polyethylene discs are used to fix the metal panels. The parasitic metal patch consists of a copper-coated plastic sheet based on 3D printing. The pair of metal panels can be placed symmetrically or combined into a larger arc-shaped parasitic metal panel. The working mechanism is that the arc-shaped metal panel is similarly equivalent to the perfect electrical conductor and located along the circular feeding substrate. The perfect electrical conductor achieves the pattern reconfiguration through the interference of the radiation in z-axis. So different combinations of arc-shaped parasitic metal panels result in rich pattern radiation states.

States	Position of the Metal Panels	Deviation Angle	Radiation Pattern (z-axis)
State I	Left 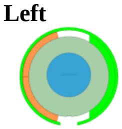	+24° (Phi=90°)	Phi=90° 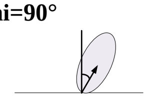
State II	Symmetry 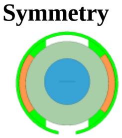	0° (Phi=90°)	Phi=90° 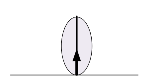
State III	Right 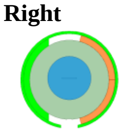	-24° (Phi=90°)	Phi=90° 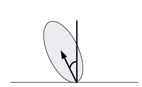
State IV	Front 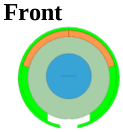	+18° (Phi=0°)	Phi=0° 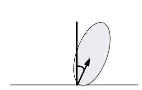
State V	Back 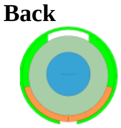	-18° (Phi=0°)	Phi=0° 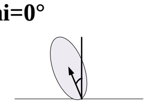

Fig. 3. The configuration and radiation pattern of the antenna in different operating states.

Firstly, Fig. 3 illustrates the three states for H-plane pattern reconfiguration, which involve the placement of the metal panels on the left, right, and both sides (State I-III). Fig. 4(a) shows the radiation pattern of the H-plane in three states, which achieves +24°, 0°, -24° radiation, respectively, while the radiation pattern in E-plane maintain the +*z*-axis direction. The maximum gain of the antenna in three states are 10.6 dBi, 8 dBi, 10.6 dBi. When the arc-shaped parasitic metal panels are placed at the front and rear side (State IV-State V) of the antenna in Fig. 3, the radiation patterns of the antenna can be controlled in E-plane, which achieves ±18° radiation in Fig. 4(b) and the radiation patterns in H-plane maintain the +*z*-axis direction. The maximum gains of the antenna in State IV and State V are 8.5 dBi. Furthermore, the beam scanning capability can be achieved by rotating the arc-shaped parasitic metal panels to alter the radiation pattern. It can achieve 360° radiation characteristics with a certain deflection angle in the +*z*-axis beam scanning.

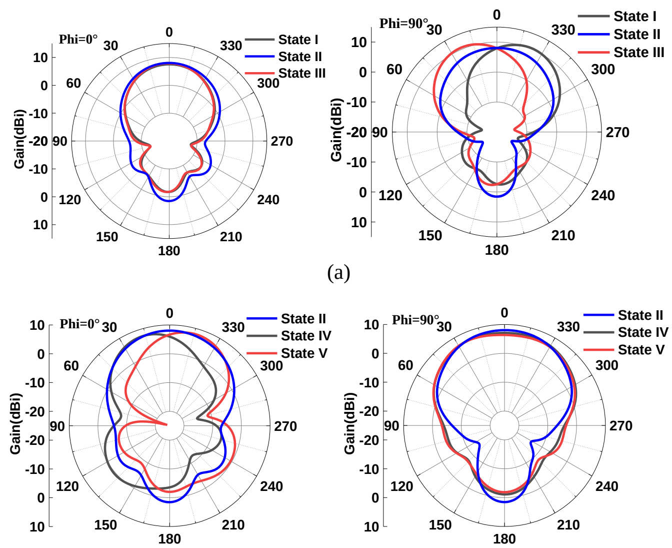

Fig. 4. The radiation pattern of the antenna in different states at 2.45GHz:(a) States I, II, III (b) States II, IV, V.

C. Beamwidth Reconfigurable Antenna Design

In addition, the beamwidth can be reconfigured by rotating the arc-shaped parasitic metal panels placed symmetrically. It can be seen from Fig. 5, when the rotation angle of the metal panels *Ro* is in the range of 0°-45°, the HPBW of the antenna changes from 48° to 79° in E-plane, while HPBW of the antenna in H-plane barely changes. Since the change of radiation pattern is caused by the arc-shaped parasitic metal panels rather than the feed network structure which will reduce the overlapped fractional bandwidth. The proposed pattern reconfigurable CDRA has a high overlapped bandwidth in different states. When the rotation angle is 0-45°, the overlapped bandwidth of the antenna is 2.34-2.71GHz. Fig. 5 also shows the impedance bandwidth in pattern/HPBW reconfigurable states. The bandwidth of the overall radiation states (State I-V and *Ro*= 0°, 30°,45°) is almost the same.

In antenna theory [21][22], the HPBW is related to the directivity D or gain G, and the directivity D is directly related to the effective antenna aperture A_e. In our design, the parasitic metal panels are equivalent to the metal electric walls, and their function is mainly to constrain the electric field vector of *xoy* plane (which is consistent with the polarization direction of the DRA), which is concentrated along the center, and enlarge the effective antenna aperture A_e. When the rotation angle *Ro* of the parasitic metal panels increases from 0° to 45°, the position of the electric wall is no longer parallel to the polarization electric field of the antenna, the component perpendicular to the polarization electric field increases. Therefore, the field constraint of the E-plane is enhanced and the effective antenna aperture A_e will be further enlarged, so the beamwidth of the E-plane will be narrower. Moreover, the gain of an antenna depends on both its directivity and its efficiency. As the component perpendicular to the polarization electric field increases, the efficiency factor of antenna k is reduced, and the antenna gain is correspondingly slightly decreased. To verify the proposed working mechanism, the electric field of the E-plane of the antenna at different rotation angles is analyzed, as shown in the Fig. 5(e). It can be seen that with the increase of *R*o, the effective antenna aperture A_{em} is increased and the field intensity in the aperture gradually decreases, and then the HPBW can be adjusted.

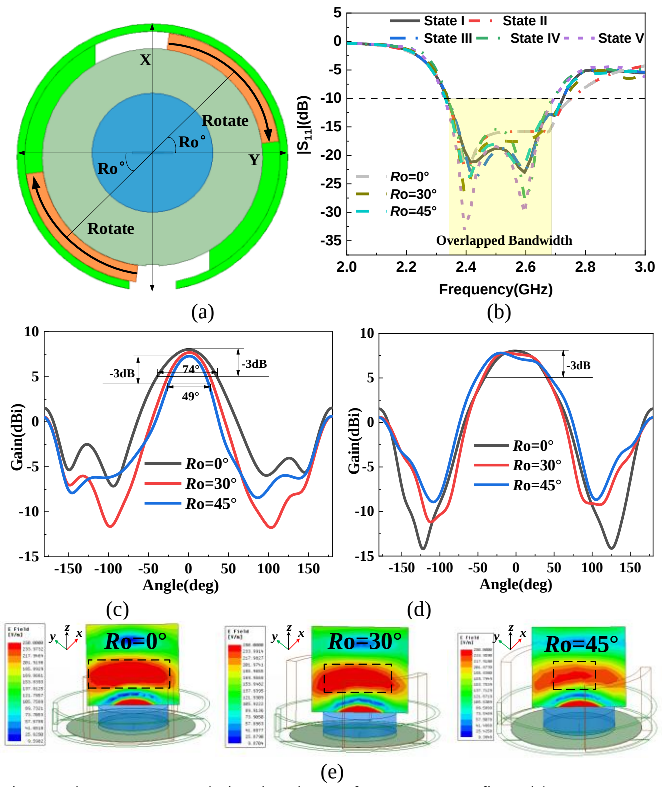

Fig. 5. The structure and simulated S_{11} of HPBW reconfigurable antenna and effect of rotation angle *Ro* on HPBW of antenna: (a) Structure (b) Simulated S_{11} (c) E-plane at 2.45GHz (d) H-plane at 2.45GHz, (e) Electric field of the antenna's E-plane in different rotation angles at 2.45GHz.

III. RESULTS AND DISCUSSION

A. Antenna Prototype and Control Scheme

For demonstration, the proposed CDRA is designed, fabricated and measured. The CDRA is made of 92% alumina ceramic and FR4 with the relative permittivity ε_r =9.5 and 4.4, and the dielectric substrate is made of Rogers 4350B with the relative permittivity ε_r =3.48, a thickness of t = 0.762 mm, and $tan\delta$ = 0.004. Fig. 6 shows photographs of the prototype. The antenna is attached to the dielectric substrate by a low relative permittivity glue.

As shown in Fig. 6, the rotation of the parasitic panels is controlled by a steerable damping shaft. Two arms of the steerable damping shaft are directly connected to the parasitic panels through the plastic brackets, and the center of the shaft is installed on the stepper motor to achieve the same rotation angle between the parasitic panel and the stepper motor. The controller provides the control signals, while the motor driver receives the signals and drives the motor, and the microcontroller controls the motor by utilizing the driver TB6600. It is worth noting that the position of the two arms of the steerable damping shaft can be adjusted. When the motor torque reaches a certain value, the two parasitic metal walls come into contact. If the motor torque does not reach a certain value, the two arms of the steerable damping shaft will not be angularly offset, so it can meet all the state of the proposed antenna in this paper. The rotation angle of the parasitic panel is controlled by a steerable stepper motor 42BYGH34, which can achieve a minimum step speed of 1.8°. The parasitic panels can rotate 360° through 200 steps, and the rotation accuracy of the stepper motor is controlled within ± 5% (± 0.09 °). The speed of AC asynchronous motor is mainly determined by the number of poles and the frequency of power supply. In theory, the synchronous speed of the bipolar motor is 3000 RPM, and the practical speed is about 2800 RPM, which can fully meet the rotation requirements. It can be applied in many potential working scenarios, such as wall-mounted antennas for indoor spaces radiation coverage, and transmitter antennas for microwave wireless power transmission application.

B. Measured and Simulated Results

The measured result for the input reflection coefficient is performed by using an Agilent vector network analyzer. Fig. 6 shows the simulated and measured reflection coefficients of the CDRA in different radiation states. First, the measured reflection coefficients of the proposed Antenna are all better than –10 dB over 2.17–2.72 GHz (simulated 2.34-2.7 GHz), which covers the 2.4 GHz band for the ISM band applications. It is verifiable that the measured results are basically consistent with the simulated results. The deviation of the scattering coefficients between simulation and measurement is mainly due to the fabrication tolerance and assembly error.

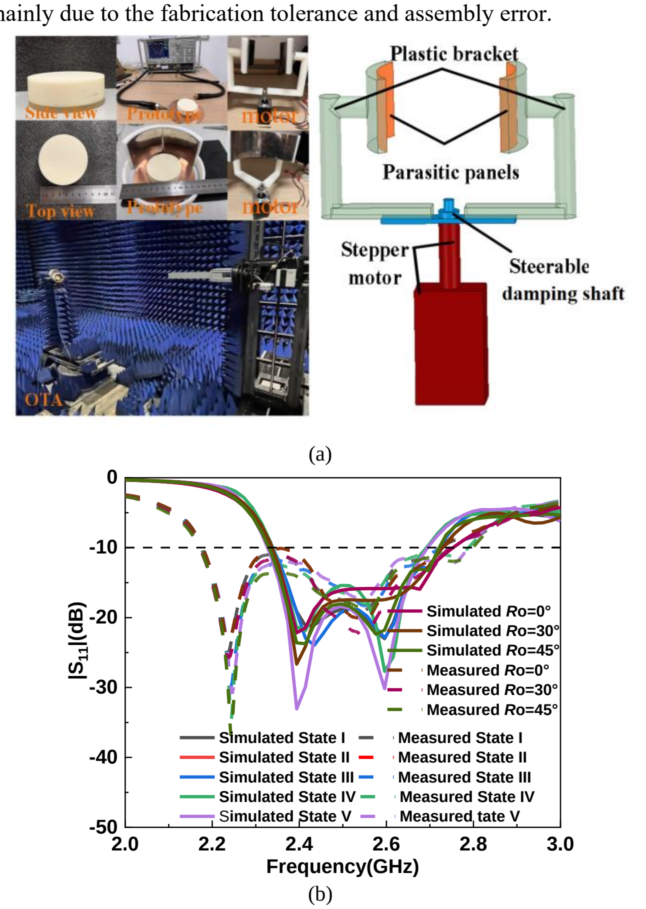

Fig. 6. (a) Photographs and (b) S_{11} of the proposed fabricated prototype.

Next, the measured maximum gains of the antenna in states I-V are 10.42 dBi (+20°), 8.24 dBi (-18°), 10.57 dBi (0°), 7.56 dBi (+17°), 7.28 dBi (-19°), respectively, which verify the high gain performance is introduced by stacked structure and radiation patterns are controlled by the parasitic metal panels. In order to confirm the radiation pattern in different states, the measured and simulated different radiation states of the CDRA in the *xoz* plane and *yoz* plane at 2.45 GHz are shown in Fig. 7(a) and (b).

Ultimately, as shown in Fig. 7(c), when the rotation angles of the metal panels *Ro* are 0°, 30°, 45°, respectively, the measured HPBW of the antenna are 90°, 56°, 49° (simulated 48°-79°) in E-plane, which indicates the HPBW reconfigurable is achieved by rotating the metal panels.

Table I reports the performance comparison between the proposed antenna and pattern reconfigurable DRAs available in the literature. Compared with Ref [5] and [14], the proposed antenna achieves a smaller size and does not need the antenna array to realize the high gain. Although the DRA of Ref [6] realizes high gain, the working band is only 1.38%. Refs. [7], [8] and [16] also have the shortcoming of narrow band, and lower gain. From table I, it can be seen that the proposed antenna has advantages of high gain, pattern-reconfigurable, compact size, simple structure and wide overlapped bandwidth. Although the angle of radiation deflection is not so large in the radiation pattern, it can be improved by reducing the distance between the antenna and the arc-shaped parasitic metal panels. While the performance of the impedance bandwidth will be affected at the same time. Furthermore, it is worth mentioning that the proposed antenna can also realize the effect of reconfigurable beamwidth.

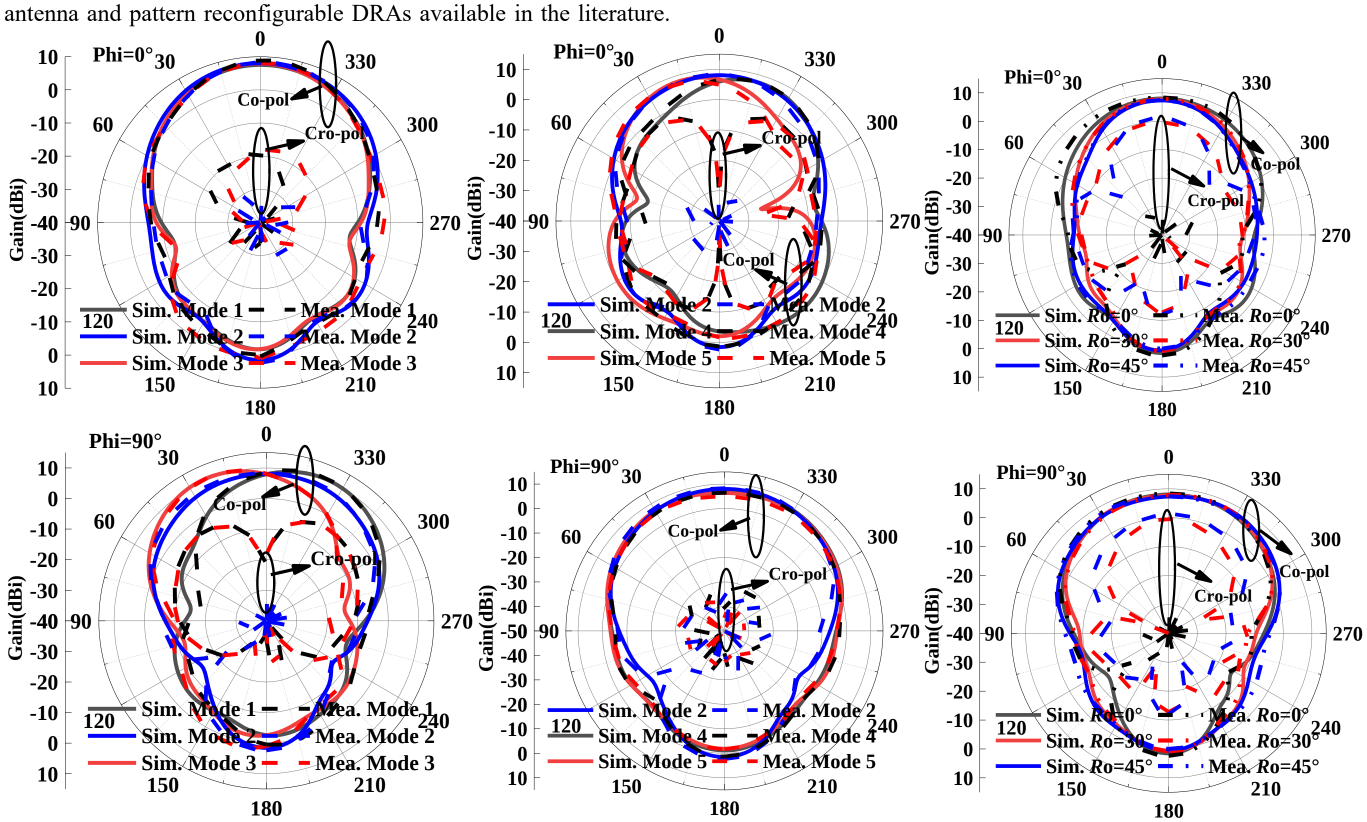

(a) (b) (c)

Fig. 7. Simulated and measured radiation patterns of the CDRA at 2.45GHz: (a) States I, II, III (Phi=0° and Phi=90°). (b) States II, IV, V (Phi=0° and Phi=90°). (c) rotation angle *Ro* (Phi=0° and Phi=90°).

TABLE I
COMPARISON BETWEEN THE PERFORMANCE OF THE PROPOSED ANTENNA WITH THOSE AVAILABLE IN THE LITERATURE

Reference	Frequency (GHz)	No. of element	Overlapped FBW (%)	Reconfiguration	Gain (dBi)	Beam Num.	Size (λ_0^3)
[5]	3	4	3.33%	electrical phase control	7.22	scanning	2.23×0.7×0.23
[6]	5.78	1	1.38%	port control	9.12	3	0.96×0.96×0.53
[7]	5	1	1.4%	pin diode	4.8	3	0.57×0.46×0.11
[8]	2.43	1	6.2%	electrical phase control	5	3	1.05×1.05×0.25
[14]	15	6	18%	port control	12.8	3	3×1.25×NA
[15]	2.4	1	2.08%	pin diode	5.3	9	0.68×0.55×0.09
[16]	2.46	1	7.3%	pin diode	5.18	3	0.27×0.27×0.2
Proposed	2.44	1	22.49%	mechanical control	10.57	scanning	0.53×0.53×0.55

λ_0 is the wavelength in free space at the center frequency of working frequency band.

IV. CONCLUSION

In this paper, a novel pattern/beamwidth reconfigurable high gain CDRA is proposed. The pattern/beamwidth reconfigurable structure is controlled by a pair of 3D-printed arc-shaped parasitic metal panels without electrical control, which can realize the high-gain beam scanning with ±18° (E-plane) and ±17° (H-plane) radiation, respectively. Moreover, the HPBW of the antenna can be changed by rotating the metal panels from 49° to 90° in the E-plane. A good agreement between simulation and measurement is achieved. The proposed CDRA realizes the measured maximum gain of 10.57 dBi at working bandwidth by the stacked structure which excites the higher order mode. Finally, the proposed antenna achieves the measured FBW of 22.49% (center frequency of 2.44GHz) which can be used for ISM band communication.

REFERENCES

[1] C. G. Christodoulou, Y. Tawk, S. A. Lane and S. R. Erwin, “Reconfigurable Antennas for Wireless and Space Applications,” *Proceedings of the IEEE*, vol. 100, no. 7, pp. 2250-2261, July 2012.

[2] J. Costantine, Y. Tawk, S. E. Barbin and C. G. Christodoulou, "Reconfigurable Antennas: Design and Applications," *Proceedings of the IEEE*, vol. 103, no. 3, pp. 424-437, March 2015.

[3] M. Li, S. -Q. Xiao and B. -Z. Wang, "Investigation of Using High Impedance Surfaces for Wide-Angle Scanning Arrays," *IEEE Transactions on Antennas and Propagation*, vol. 63, no. 7, pp. 2895-2901, July 2015.

[4] Z. Wang, P. S. Hall, J. R. Kelly and P. Gardner, “Wideband Frequency-Domain and Space-Domain Pattern Reconfigurable Circular Antenna Array,” *IEEE Transactions on Antennas and Propagation*, vol. 65, no. 10, pp. 5179-5189, Oct. 2017.

[5] Y. -F. Cheng, X. Ding, W. Shao and B. -Z. Wang, "Dual-Band Wide-Angle Scanning Phased Array Composed of SIW-Cavity Backed Elements," *IEEE Transactions on Antennas and Propagation*, vol. 66, no. 5, pp. 2678-2683, May 2018.

[6] X. Yang, Y. Liu, H. Lei, Y. Jia, P. Zhu and Z. Zhou, "A Radiation Pattern Reconfigurable Fabry–Pérot Antenna Based on Liquid Metal," *IEEE Transactions on Antennas and Propagation*, vol. 68, no. 11, pp. 7658-7663, Nov. 2020.

[7] C. Fan, B. Wu, Y. Hu, Y. Zhao and T. Su, "Millimeter-Wave Pattern Reconfigurable Vivaldi Antenna Using Tunable Resistor Based on Graphene," *IEEE Transactions on Antennas and Propagation*, vol. 68, no. 6, pp. 4939-4943, June 2020.

[8] W. Li, Y. Zhao, X. Ding, L. Wu and Z. Nie, "A Wideband Pattern-Reconfigurable Loop Antenna Designed by Using Characteristic Mode Analysis," *IEEE Antennas and Wireless Propagation Letters*, vol. 21, no. 2, pp. 396-400, Feb. 2022.

[9] Z. Chen, Z. Song, H. Liu, X. Liu, J. Yu and X. Chen, "A Compact Phase-Controlled Pattern-Reconfigurable Dielectric Resonator Antenna for Passive Wide-Angle Beam Scanning," *IEEE Transactions on Antennas and Propagation*, vol. 69, no. 5, pp. 2981-2986, May 2021.

[10] B. K. Ahn, H. -W. Jo, J. -S. Yoo, J. -W. Yu and H. L. Lee, "Pattern Reconfigurable High Gain Spherical Dielectric Resonator Antenna Operating on Higher Order Mode," *IEEE Antennas and Wireless Propagation Letters*, vol. 18, no. 1, pp. 128-132, Jan. 2019.

[11] Y. -H. Ke, L. -L. Yang and J. -X. Chen, "A Pattern-Reconfigurable Dielectric Resonator Antenna Based on Switchable Directors," *IEEE Antennas and Wireless Propagation Letters*, vol. 21, no. 3, pp. 536-540, March 2022.

[12] X. Liu, K. W. Leung, T. Zhang, N. Yang, P. Gu and R. Chen, "An Electrically Controlled Pattern- and Polarization-Reconfigurable Cylindrical Dielectric Resonator Antenna," *IEEE Antennas and Wireless Propagation Letters*, vol. 20, no. 12, pp. 2309-2313, Dec. 2021.

[13] J. Ren et al., "Radiation Pattern and Polarization Reconfigurable Antenna Using Dielectric Liquid," *IEEE Transactions on Antennas and Propagation*, vol. 68, no. 12, pp. 8174-8179, Dec. 2020.

[14] N. H. Shahadan, M. H. Jamaluddin, M. H. Dahri, M. R. Kamarudin and K. H. Yusof, "High Gain Switchable Dielectric Resonator Antenna Array for 5G Applications," 2018 International Symposium on Antennas and Propagation (ISAP), pp. 1-2, Oct. 2018.

[15] J. -X. Chen, Y. -H. Ke, L. -L. Yang and W. -W. Yang, "Pattern-Reconfigurable Dielectric Resonator Antenna With Endfire Beam-Scanning Feature," *IEEE Antennas and Wireless Propagation Letters*, vol. 21, no. 7, pp. 1398-1402, July 2022.

[16] X. Liu, K. W. Leung and N. Yang, "A Pattern-Reconfigurable Cylindrical Dielectric Resonator Antenna with Three Switchable Radiation Patterns," *IEEE Transactions on Antennas and Propagation*, early access, doi: 10.1109/TAP.2023.

[17] T. Govindan et al. "A Design and Analysis of a Conformal MIMO Ingestible Bolus Sensor Antenna for Wireless Capsule Endoscopy for Animal Husbandry", *IEEE Sensors Journal,* Vol. 23, No. 22, pp. 28150 -28158, 2023

[18] J. T. H. St-Martin, Y. M. M. Antar, A. A. Kishk, A. Ittipiboon and M. Cuhaci, "Aperture-coupled dielectric resonator antenna," *Antennas and Propagation Society Symposium 1991 Digest*, vol.2, pp. 1086-1089 1991.

[19] D. Guha, A. Banerjee, C. Kumar and Y. M. M. Antar, "Higher Order Mode Excitation for High-Gain Broadside Radiation From Cylindrical Dielectric Resonator Antennas," *IEEE Transactions on Antennas and Propagation*, vol. 60, no. 1, pp. 71-77, Jan. 2012.

[20] A. W. Glisson, D. Kajfez and J. James, "Evaluation of Modes in Dielectric Resonators Using a Surface Integral Equation Formulation," *IEEE Transactions on Microwave Theory and Techniques*, vol. 31, no. 12, pp. 1023-1029, Dec. 1983.

[21] D. Kajfez, A. W. Glisson and J. James, "Computed Modal Field Distributions for Isolated Dielectric Resonators," *IEEE Transactions on Microwave Theory and Techniques*, vol. 32, no. 12, pp. 1609-1616, Dec. 1984.

[22] J. D. Kraus, Antennas, Mcgraw-Hill 2nd Edition, 1988.

[23] C. A. Balanis, Antenna Theory: Analysis and Design, 4th Edition, 2016.